

Stability of slope along steep road in Abha, Asir Region, Kingdom of Saudi Arabia

SAIFUL ISLAM^{1,*}, RINI ASNIDA ABDULLAH¹, JAVED MALICK², MOHD AHMED²

¹ Faculty of Civil Engineering, Universiti Teknologi Malaysia, Johor, Malaysia

² Department of Civil Engineering, King Khalid University, Kingdom of Saudi Arabia

*Corresponding author email address: isaiful2@graduate.utm.my

Abstract: Slope stability plays a vital role in steep mountainous slopes. The main aim of this study is to investigate the slope stability of an area located along a steep road in Abha, Asir Region, Saudi Arabia using numerical simulation software -FLAC -3D. The area is frequently facing problems of slope failure due to various factors, including heavy rainfall, faulting planes, shear zones, weak rocks, narrow road sections with horizontal and vertical curves, and anthropogenic activities as well. The geotechnical parameters required as input data is determined from laboratory testing. From the analysis it was observed that the maximum displacement computed in the slope in the x-direction is 0.0162 m and the specific maximum displacement computed in the slope in the z-direction is 0.166 m. The analysis of XX stress shows that the tensile stress occurred along the top of the slope and its value is 45.68 kPa. While analysis of YY stress shows that the tensile stress occurred along the top of the slope and its value is 15.43 kPa. Similarly, it can be seen from the figure of ZZ stress contour that the tensile stress occurred along the top of the slope with value of 15.75 kPa. It was observed that negligible deformation occurred in the y-direction. The places at which the value of factor of safety showed less than one confirms instability.

Keywords: Slope stability, numerical simulation, factor of safety, failure surface

INTRODUCTION

In Asir Region, most of the road and highway constructions require significant rock cutting operations as these roads pass through complex terrains. Most of the cutting operations are generally done by blasting and mechanical excavation which in turn give rise to highly unstable slopes containing many weak zones. The climate in Asir Region is characterised by significant rainstorms during summer season, resulting in deterioration of the rock cuts and subsequently rendering the area as vulnerable due to high slope failures.

Currently, the problem of slope failures has become predominant due to anthropogenic activities (i.e. road cutting operations) and the development of the area for housing purposes, large infrastructures and quarries as well (Alemdag *et al.*, 2014). The rock slope instability is mostly caused by poor blasting operations, adverse changes in climate, and presence of discontinuities in the slopes (Li *et al.*, 2009). Thus, it is very important to know the orientation, nature and properties of discontinuities and also the geological parameters and properties of intact rocks during slope stability investigations (Singh *et al.*, 2013). Moreover, earthquake activities or high groundwater pressures (after rainstorms) will also lead to high risk of slope failures (Youssef & Maertz, 2013; Zhou *et al.*, 2013; Bai *et al.*, 2014; Igwe, 2015). The literal meaning of slope stability is the resistance of an inclined block to sliding or to collapse along a slip surface (Youssef *et al.*, 2015). Several researchers (Goodman,

1989; Pettifer & Fookes, 1994; Wyllie & Mah, 2014) developed various important methods to analyze unstable slopes such as limit equilibrium approach, kinematical method and most predominantly the numerical technique. Kinematical analysis deals with only movement of slopes consisting of blocks without taking into account the forces that cause the block to move. Meanwhile, limit equilibrium approach considers various important parameters such as the shear strength of rock, intrinsic and external forces. On the contrary, numerical analysis are done in order to verify and check the results obtained through kinematic and limit equilibrium approaches (Gurocak *et al.*, 2008). Hence, we can say that the numerical method proves to be a very important tool for slope stability analysis and currently, numerical techniques such as FEM, FDM, and DEM are the popular techniques to judge slope stability (Verma & Singh, 2010; Sarkar *et al.*, 2012).

In this present study, Flac 3d is the numerical technique used to check the stability of a vulnerable slope by computing displacements in different directions. The factor of safety is also computed in order to determine the unstable region in the slope.

STUDY AREA

The study area is located in the southern most mountainous part of Samma escarpment road that lies in Asir Province of Kingdom of Saudi Arabia, shown in Figure 1. The weather is characterized by substantial rainstorm during summer seasons; and this leads to

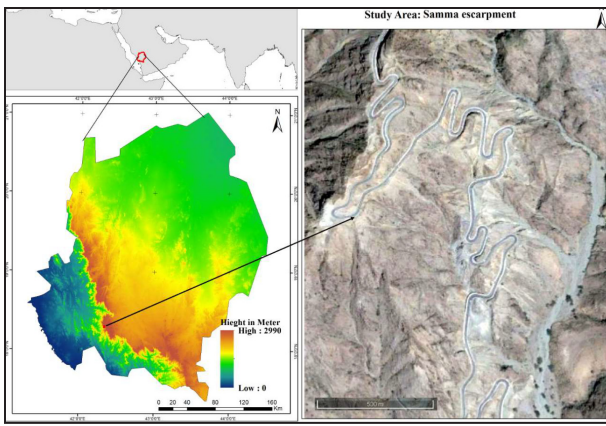


Figure 1: Location map for Samma escarpment region.

deterioration of the rock cuts and creating areas that are prone to slope failures. Currently these escarpment roads that are one of the passages connecting villages and cities such as Abha and Baha are facing rockslide problems.

As far as geological aspect is concern, the bedrock outcropping along the Samma road comes under Neoproterozoic Bahah Group. The dominant rock type is light-to-dark-colored phyllites (meta-mudstones and meta-siltstones) interbedded with massive graywackes, black graphitic slates, and cut by concordant diabase sills. Phyllites are commonly laminated and have well developed metamorphic foliations (parallel to bedding). Another structure that had originated after a large-scale folding activity is low-angle thrust faults (Youssef *et al.*, 2015).

NUMERICAL MODELING

The purpose of implementing the Flac-3D software is to solve various problems related to geo-mechanics (Itasca, 2003). Three-dimensional nonlinear analysis scheme is used by implementing the finite difference code *Flac-3D* to study the slope of Samma escarpment road. *Flac-3D* exhibit self-generating 3D grid generator capabilities. The grids are generated by defining pre-defined shapes such as brick, wedge, pyramid and cylinder.

In the present study, the geometrical slope has been created by making use of a number of brick shape elements and one wedge element at the bottom edge. Figure 2 shows the element numbering for the brick shape used for creating the soil domain. In this figure, p0, p1....p7 specify the reference (corner) points of the shapes, n1, n2 and n3 specify the number of zones in their respective directions and r1, r2 and r3 specify the ratios that is used to space the zones with increasing or decreasing geometric ratio. Similarly Figure 3 shows the wedge element that is used to create the hill toe.

The geometry of the slope obtained from the wedge and brick shapes is described as 100 m in the x-direction and 10 m in the y-direction, while in the z-direction it fluctuates from 0 to 60 m depending upon the variation of the slope. The bottom plane of the grid is restrained against movement. The plane at x = 0 m is restricted in

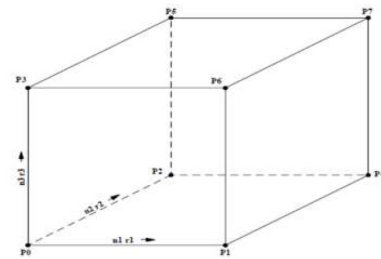


Figure 2: Brick element.

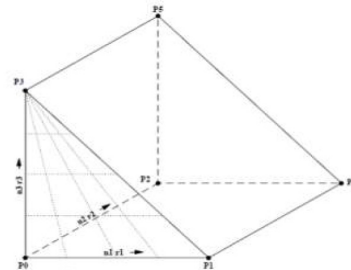


Figure 3: Wedge element.

the x-direction while movement is allowed in the y- and z-directions. Similarly, for planes at y= 0 and y= 10 m, the restriction is also in the y-direction while movements are allowed in the x- and z-directions. The parameters used for the soil modeling obtained from geotechnical test are summarized in Table 1. The model chosen for the slope modelling is Mohr-Coulomb plasticity model while the input values required are cohesion and internal friction angles, shear modulus, bulk modulus, and density. The slope geometry and displacement contours are shown in Figure 4 and 5 respectively.

The Mohr-Coulomb plasticity model is described by the relation as shown below:

$$F_s = \sigma_1 - \sigma_3 N_\phi + 2c\sqrt{N_\phi} \tag{1}$$

$$\text{Where } N_\phi = ((1+\sin_\phi))/((1-\sin_\phi)) \tag{2}$$

- σ_1 = Major Principal stress;
- σ_3 = Minor Principal stress;
- ϕ = Angle of internal friction;
- c = cohesion

The first step in the analysis approach is the generation of a grid. Once the grid is generated for the soil medium, the model is assigned an appropriate model (Mohr-Coulomb in this case). To bring it to an equilibrium stress-state, the gravitational loading was then applied.

Table 1: Input parameters.

Density(kg/m ³)	1850
Poissons Ratio	0.25
Shear Modulas (N/m ²)	56*10 ⁶
Bulk Modulas (N/m ²)	93.3*10 ⁶
Cohesion (N/m ²)	10*10 ⁴
Internal friction Angle	35°

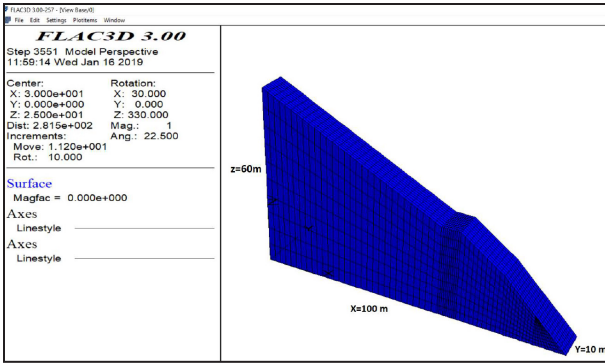


Figure 4: Slope geometry.

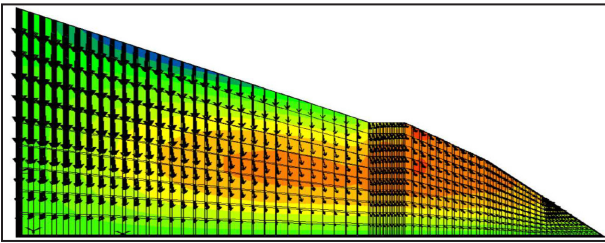


Figure 5: Displacement contour.

The slope model will attain its equilibrium condition when each grid point net nodal force vector reaches zero. However, in numerical simulation the maximum unbalanced forces will not reach zero but it is assumed to be in an equilibrium state when the maximum unbalanced force is negligibly small compared to the total applied force. The safety factor (FOS) computed by Zheng *et al.* (2005) is the ratio of total resisting forces to total driving forces along a certain slip line:

$$FOS = \tau / \tau_s \quad (3)$$

where, τ_s = shear stress, τ = shear strength given by:

$$\tau = c + \sigma_n \tan \phi \quad (4)$$

where c = cohesion, σ_n = total normal stress, and ϕ = effective angle of internal friction

RESULTS AND DISCUSSIONS

The slope stability analysis results show that the maximum value of displacement magnitude is 16.62 cm, that occurred at the top of the heel side. The x-displacement contour (Figure 6) shows that the displacement occurred at the downslope, just adjacent to the road and its value was observed to be 1.62 cm. It can be seen that the y-displacement (Figure 7) showed almost negligible values. Moreover, from the displacement vector figure it can be concluded that the soil at the downslope is sliding forward whereas settlement is observed at the upstream slope. The maximum value of the z-displacement (Figure 8) is observed to be 16.62 cm. From the analysis it can also be observed that the maximum displacement computed in the slope in the x-direction is 0.0162 m and the specific maximum displacement computed in the slope in the z-direction is 0.166 m. The analysis of XX

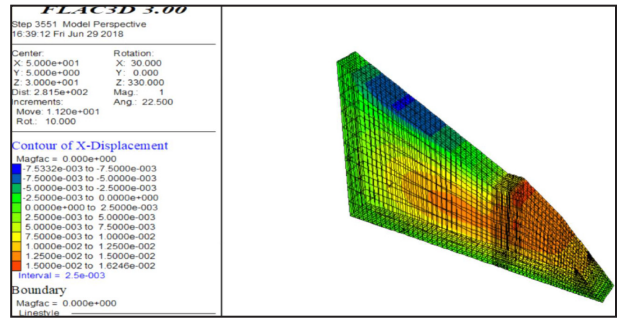


Figure 6: X-displacement contour.

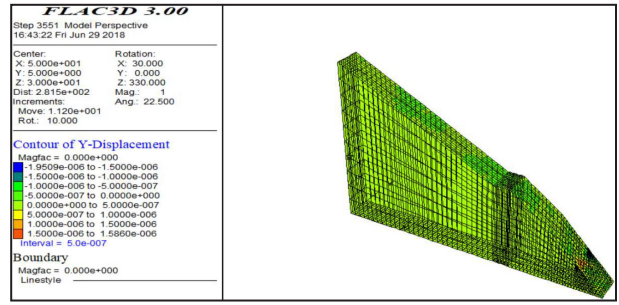


Figure 7: Y-displacement contour.

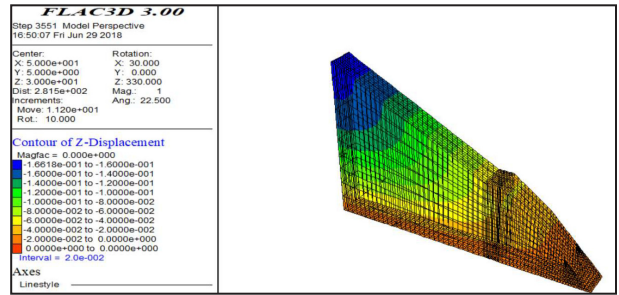


Figure 8: Z-displacement contour.

stress (Figure 9) showed that the tensile stress occurred along the top of the slope and its value is 45.68 kPa. While analysis of YY stress (Figure 10) showed that the tensile stress occurred along the top of the slope and its value is 15.43 kPa. (Figure 11). It can be noted that negligible deformation occurred in the y-direction. The factor of safety was computed at critical sections at $x = 0, 20, 40, 60, 66, 80, 90$ and 95 m respectively and with a difference of 5 m in the z-direction as shown in Figure 12 to judge the state of the slope. The slope besides the road at $x = 66$ m was found to be critical as the factor of safety is less than one. The places at which the factor of safety values is less than one confirms instability. Also, the plotted contour of FOS with reference to elevation and height indicates that it is unstable at higher heights while stable at lower heights. The contours also show trends of a circular failure.

CONCLUSION

The research work deals with stability of slope by computing the displacement, stress and factor of safety in three directions along the Samma escarpment road in Asir Region, Kingdom of Saudi Arabia. In this region

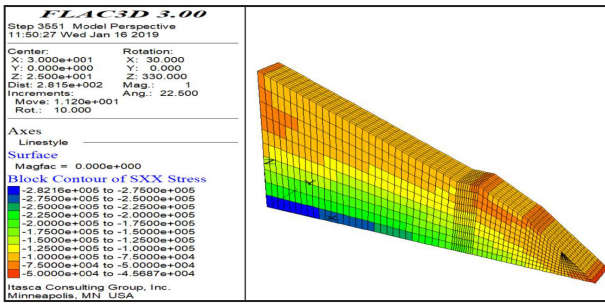


Figure 9: Stress in xx-direction.

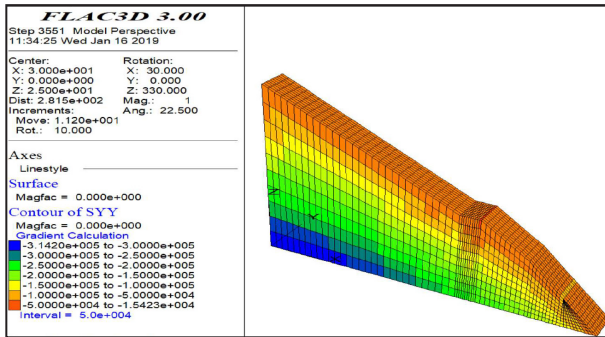


Figure 10: Stress in yy-direction.

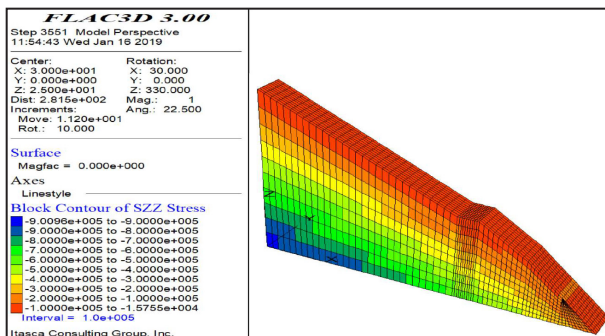


Figure 11: Stress in zz-direction.

and particularly along the escarpment road, the problem of landslides and erosion features are most common which renders not only human lives under threat, but also triggering huge damages to highway and infrastructures. The slope stability analysis was performed by making use of a three-dimensional finite difference codes. From the analysis it was observed that the maximum displacement computed in the slope in the x-direction is 0.0162 m and the specific maximum displacement in the z-direction is 0.166 m. However, in the y-direction the deformation is almost negligible. The maximum stresses in the x-, y- and z-directions are at the top of slope surface. Thus, we can definitely conceive that the slope is undergoing large deformations which is found to be a circular failure. The places where the factor of safety values is less than one confirms instability. The slope is quite stable at lower heights, as shown by the factor of safety values. The factor of safety then decreases because of positive shear strain rate and further increases at higher heights because of negative shear strain rate. Hence it can be concluded that

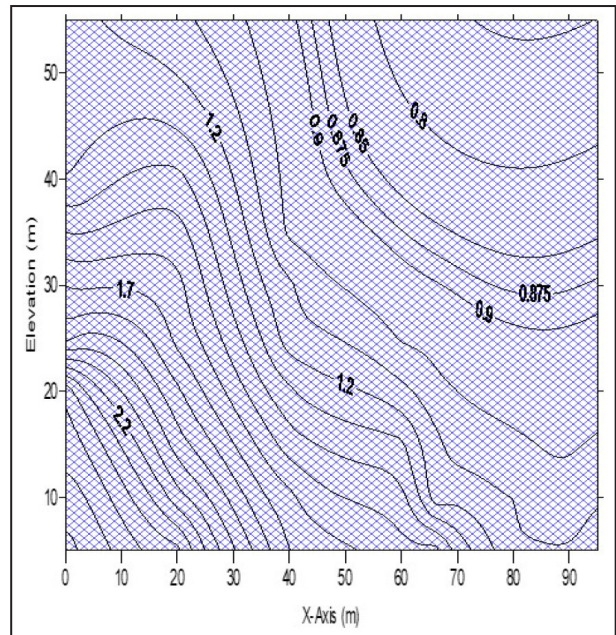


Figure 12: Contour of Factor of Safety with reference to elevation and x-axis.

there are deformations at the Samma escarpment road and analysis results show that the slope is critically unsafe.

ACKNOWLEDGEMENTS

The authors of current work wish to thank Universiti Teknologi Malaysia, Johor Bahru for their facilities and support. We would also like to thank King Khalid University, Abha, Asir Region, Saudi Arabia for providing the lab support.

REFERENCES

Alemdag, S., A. Akgun, A. Kaya, & C. Gokceoglu, 2014. A large and rapid planar failure: causes, mechanism, and consequences (Mordut, Gumushane, Turkey). *Arabian Journal of Geosciences*, 7 (3), 1205-1221.

Bai, S. B., J. Wang, B. Thiebes, C. Cheng, & Z. Y. Chang, 2014. Susceptibility assessments of the Wenchuan earthquake-triggered landslides in Longnan using logistic regression. *Environmental Earth Sciences*, 71 (2), 731-743.

Goodman, Richard E., 1989. *Introduction to rock mechanics*, Vol. 2. Wiley, New York. 576 p.

Gurocak, Zulfu, Selcuk Alemdag, & Musharraf M. Zaman, 2008. Rock slope stability and excavatability assessment of rocks at the Kapikaya dam site, Turkey. *Engineering Geology*, 96 (1-2), 17-27.

Igwe, O., 2015. Analyses of the October 2013 fatal slope failures on the metamorphic terrains of Obudu tourist area, South-Southeast Nigeria. *Arabian Journal of Geosciences*, 8 (9), 7425-7434.

Itasca, 2003. *PFC3D User's Manual*, Version 3.0. Itasca Consulting Group Inc, Minneapolis, MN, USA.

Li, Z. H., H. W. Huang, Y. D. Xue, & J. Yin, 2009. Risk assessment of rockfall hazards on highways. *Georisk*, 3 (3), 147-154.

Maerz, Norbert H., Ahmed M. Youssef, Biswajeet Pradhan, & Ali Bulkhi, 2015. Remediation and mitigation strategies for rock fall hazards along the highways of Fayfa Mountain, Jazan Region, Kingdom of Saudi Arabia. *Arabian Journal*

- of Geosciences, 8 (5), 2633-2651.
- Pettifer, G. S., & P. G. Fookes, 1994. A revision of the graphical method for assessing the excavatability of rock. Quarterly Journal of Engineering Geology and Hydrogeology, 27 (2), 145-164.
- Sarkar, Kripamoy, T. N. Singh, & A. K. Verma, 2012. A numerical simulation of landslide-prone slope in Himalayan region - A case study. Arabian Journal of Geosciences, 5 (1), 73-81.
- Singh, T. N., S. P. Pradhan, & V. Vishal, 2013. Stability of slopes in a fire-prone mine in Jharia Coalfield, India. Arabian Journal of Geosciences, 6 (2), 419-427.
- Verma, Amit K., & T. N. Singh, 2010. Assessment of tunnel instability - A numerical approach. Arabian Journal of Geosciences, 3 (2), 181-192.
- Wyllie, Duncan C. & Chris Mah, 2014. Rock slope engineering. CRC Press, London, New York. 456 p.
- Youssef, Ahmed M., & Norbert H. Maerz, 2013. Overview of some geological hazards in the Saudi Arabia. Environmental Earth Sciences, 70 (7), 3115-3130.
- Youssef, Ahmed M., Biswajeet Pradhan, & Saad G. Al-Harathi, 2015. Assessment of rock slope stability and structurally controlled failures along Samma escarpment road, Asir Region (Saudi Arabia). Arabian Journal of Geosciences, 8 (9), 6835-6852.
- Zheng, Hong, D. F. Liu, & Chun Guang Li, 2005. Slope stability analysis based on elasto-plastic finite element method. International Journal for Numerical Methods in Engineering, 64 (14), 1871-1888.
- Zhou, Jia-wen, Peng Cui, & Xing-guo Yang, 2013. Dynamic process analysis for the initiation and movement of the Donghekou landslide-debris flow triggered by the Wenchuan earthquake. Journal of Asian Earth Sciences, 76, 70-84.

Manuscript received 5 July 2018

Revised manuscript received 16 January 2019

Manuscript accepted 23 March 2019